moiety of pyruvate carboxylase. In principle, this value for k_4 should equal that determined from the onset of inhibition. The latter value was estimated to be less than 2×10^{-3} s^{-1}, which is consistent with the prediction.

It might be argued that the linear dependence of k' on avidin concentration is consistent with mechanism B and that the data in Figure 5 represent the lower end of a curve which would saturate at much higher concentrations of avidin. Such a proposal cannot be eliminated, but it implies that in eq 2b, $k_5 \gg k_4$ so that the proportion of the enzyme which is present as EI is extremely small. Thus the mechanism degenerates into a form which is equivalent to mechanism A. There may be, and probably are, several transient enzyme forms between E and EI, but these were not detected in the present study and should not be proposed in the absence of definitive evidence for their existence. Thus, we are inclined to accept mechanism A as an approximate description of the interaction between avidin and pyruvate carboxylase.

References

Alberty, R. A., & Hammes, G. G. (1958) *J. Phys. Chem. 62*, 154-159.

Cha, S. (1975) *Biochem. Pharmacol. 24*, 2177-2185.

Cha, S. (1976) *Biochem. Pharmacol. 25*, 1561.

Cohen, N. D., Beegen, H., Utter, M. F., & Wrigley, N. G. (1979) *J. Biol. Chem. 254*, 1740-1747.

Cornish-Bowden, A. (1975) *Biochem. J. 149*, 305-312.

Duggleby, R. G. (1980) *Eur. J. Biochem. 109*, 93-96.

Duggleby, R. G. (1981) *Anal. Biochem. 110*, 9-18.

Fall, R. R., & Hector, M. L. (1977) *Biochemistry 16*, 4000-4005.

Frieden, C. (1970) *J. Biol. Chem. 245*, 5788-5799.

Goss, N. H., Dyer, P. Y., Keech, D. B., & Wallace, J. C. (1979) *J. Biol. Chem. 254*, 1734-1739.

Green, N. M. (1965) *Biochem. J. 94*, 23c-24c.

Green, N. M. (1975) *Adv. Protein Chem. 29*, 85-133.

Green, N. M., & Toms, E. J. (1973) *Biochem. J. 133*, 687-700.

Halenz, D. R., Feng, J.-Y., Hegre, C. S., & Lane, M. D. (1962) *J. Biol. Chem. 237*, 2140-2147.

Kaziro, Y., Leone, E., & Ochoa, S. (1960) *Proc. Natl. Acad. Sci. U.S.A. 46*, 1319-1327.

Moss, J., & Lane, M. D. (1972) *J. Biol. Chem. 247*, 4944-4951.

Rylatt, D. B., Keech, D. B., & Wallace, J. C. (1977) *Arch. Biochem. Biophys. 183*, 113-122.

Scrutton, M. C., & Utter, M. F. (1965) *J. Biol. Chem. 240*, 3714-3723.

Scrutton, M. C., & Utter, M. F. (1967) *J. Biol. Chem. 242*, 1723-1735.

Scrutton, M. C., & Mildvan, A. S. (1968) *Biochemistry 7*, 1490-1505.

Utter, M. F., & Keech, D. B. (1960) *J. Biol. Chem. 235*, PC17-PC18.

Williams, J. W., & Morrison, J. F. (1979) *Methods Enzymol. 63*, 437-467.

Williams, J. W., Morrison, J. F., & Duggleby, R. G. (1979) *Biochemistry 18*, 2567-2573.

Mechanism for Catalysis and Regulation of Adenosine 5′-Triphosphate Hydrolysis by Chloroplast Coupling Factor 1†

Michael F. Bruist‡ and Gordon G. Hammes*

ABSTRACT: A comprehensive mechanism is proposed for the hydrolysis of ATP and its regulation by chloroplast coupling factor 1. In this mechanism, a regulatory site is proposed to bind nucleotides very tightly. When ADP occupies this site, the enzyme is inactive, but when ATP binds to this site, the enzyme is active. Furthermore, the rate of nucleotide dissociation from the regulatory site is greatly enhanced during ATP hydrolysis. Steady-state kinetic studies of ATP hydrolysis and the inhibition of hydrolysis by 2′(3′)-(trinitrophenyl)-ADP and -ATP reveal positive cooperativity in substrate binding at low substrate concentrations that is enhanced by the inhibitors. In terms of the proposed mechanism, this is due to the displacement of substrate from the regulatory site by inhibitors. The binding of the inhibitors is characterized by a dissociation constant in the nanomolar range. The initial rate of dissociation of ADP from the regulatory site during ATP hydrolysis has a maximum rate constant of 0.09 s^{-1} and a Michaelis constant for ATP of about 80 μM, which is similar to the apparent Michaelis constant associated with ATP hydrolysis. The binding of the substrate 1,N^6-ethenoadenosine 5′-triphosphate to a specific site on the enzyme was studied by following the time course of fluorescence quenching with the stopped-flow method. The binding process can be characterized by a mechanism in which the substrate and enzyme rapidly form a complex that undergoes a relatively slow conformational change. The rate constant characterizing the conformational change is larger than the catalytic turnover number, indicating this binding reaction can be part of the catalytic mechanism. This two-step binding process can be readily incorporated into the general mechanism proposed for ATP hydrolysis. A diverse number of other observations in the literature also are consistent with the proposed mechanism.

The coupling factor 1 (CF_1)[1] is the portion of the ATP synthesizing complex of chloroplasts that contains the catalytic site. It can be isolated as a soluble protein and is composed of five different types of subunits [cf. Baird & Hammes (1979)]. While only membrane-bound enzyme can synthesize ATP, both membrane-bound enzyme and soluble CF_1 catalyze the reverse reaction, ATP hydrolysis. The synthesis and hy-

† From the Department of Chemistry, Cornell University, Ithaca, New York 14853. *Received December 30, 1981.* This work was supported by a grant from the National Institutes of Health (GM 13292).

‡ National Institutes of Health Predoctoral Trainee (GM 07273).

[1] Abbreviations: CF_1, chloroplast coupling factor 1; EDTA, ethylenediaminetetraacetic acid; TNP-ADP and TNP-ATP, 2′,3′-*O*-(2,4,6-trinitrophenyl)adenosine 5′-diphosphate and 5′-triphosphate, respectively; ϵ-ADP and ϵ-ATP, 1,N^6-ethenoadenosine 5′-diphosphate and 5′-triphosphate, respectively; Tris, tris(hydroxymethyl)aminomethane.

0006-2960/82/0421-3370$01.25/0

drolysis of ATP, which in intact chloroplasts are coupled to the hydrogen ion gradient across the membrane, are regulated by ADP and ATP. The molecular mechanisms of synthesis and hydrolysis, coupling to the proton gradient, and regulation of synthesis and hydrolysis are still controversial [cf. Boyer et al. (1977) and Cross (1981)].

Previous studies have characterized three distinct ADP and ATP binding sites on CF_1 (Bruist & Hammes, 1981; Cerione & Hammes, 1982). These sites are designated by number as follows. Site 1 contains tightly bound ADP which is always found associated with isolated CF_1. The ADP in this site exchanges with medium ATP or ADP, but cannot be removed by dialysis or gel permeation chromatography in the absence of exogenous nucleotides. Site 2 binds ATP very tightly in the presence of Mg^{2+}; this tightly bound ATP does not dissociate during catalysis. Site 2 binds ADP with a dissociation constant of 3 μM. Site 3 can be detected with equilibrium binding techniques and has a dissociation constant of about 4 μM for ADP or ATP.

In this work, the function of these three sites has been investigated by using steady-state, stopped-flow, and nucleotide exchange kinetics. A comprehensive model is developed for the mechanism of ATP hydrolysis and its regulation. This model postulates that site 3 is the catalytic site and site 1 is an important regulatory site.

Materials and Methods

Chemicals. The ADP, ATP (vanadium free), ϵ-ADP, ϵ-ATP, bisphosphoglycerate, NAD, phosphoglycerate kinase, and glyceraldehyde-3-phosphate dehydrogenase were from Sigma Chemical Co., and TNP-ADP and TNP-ATP were from Molecular Probes. The ^3H-labeled ADP and ATP were from New England Nuclear and the ^{32}P-labeled nucleotides from Amersham Corp. Radioactive ADP was purified by paper chromatography using isobutyric acid–1 N ammonia (100:60 v/v); radioactive and nonradioactive ATP and ϵ-ATP were purified by column chromatography on Bio-Rad AG-1-X4 Cl^- anion exchange resin (Bruist & Hammes, 1981). All other chemicals were high quality commercial grades, and distilled deionized water was used for all solutions. Unless indicated, experiments were performed at room temperature, 20 ± 2 °C.

Enzyme. The CF_1 was prepared from fresh market spinach (Lien & Racker, 1971; Binder et al., 1978). Enzyme having a 305:340-nm fluorescence ratio (excitation at 280 nm) greater than 1.5 was collected and stored as an ammonium sulfate precipitate in 2 M ammonium sulfate, 10 mM Tris-HCl (pH 7.2), 1 mM EDTA, and 0.5 mM ATP. Its purity was checked by sodium dodecyl sulfate–polyacrylamide gel electrophoresis. The CF_1 was activated by heating at 60 °C for 4 min in 40 mM ATP, 30 mM Tris-HCl (pH 8.0), 7 mM dithiothreitol, and 2 mM EDTA (Farron & Racker, 1970). The specific activity immediately after activation was 8–14 μmol/(mg·min) in 50 mM NaCl, 6 mM $CaCl_2$, 1 mM EDTA, and 0.5 mM ATP at pH 8.0, 20 °C. An extinction coefficient of 0.483 cm^2/mg at 277 nm (Bruist & Hammes, 1981) and a molecular weight of 325 000 (Farron, 1970) were used for determining concentrations of CF_1.

Dissociable nucleotides were removed from CF_1 by passage through a Sephadex G-25 medium column (1 × 60 cm; Cantley & Hammes, 1975) or by ammonium sulfate precipitation followed by two or three 3-mL centrifuge columns (Penefsky, 1977) of Sephadex G-50 fine equilibrated with the appropriate buffer. Sites 1 and 2 were labeled with radioactive ADP and MgATP, respectively, as described by Bruist & Hammes (1981). Most of the experiments were done in a NaCl–Tris–EDTA buffer containing 50 mM NaCl, 10 mM Tris-HCl, and 1 mM EDTA at pH 8.0.

ATP Hydrolysis Assays. Three different assays for ATP hydrolysis were used: a spectrophotometric enzyme coupled assay, a pH-stat assay, and a [γ-^{32}P]ATP assay. In the enzyme-coupled assay (Bücher, 1947), the ADP produced by ATP hydrolysis was phosphorylated with bisphosphoglycerate by using phosphoglycerate kinase. The consumption of bisphosphoglycerate was coupled to the reduction of NAD by glyceraldehyde-3-phosphate dehydrogenase. The NAD reduction was monitored at 340 nm. Rates were calculated by using a conversion factor of $5.34A_{340}$/(μmol of ADP/mL), which was determined by the addition of known amounts of ADP to the assay mixture. Assays had a final volume of 0.5 mL and contained 50 mM NaCl, 6 mM DL-glyceraldehyde 3-phosphate, 5 mM Tris-HCl (pH 8.0), 2.5 mM $CaCl_2$, 1.5 mM NAD, 1 mM EDTA, 1 mM P_i, 24 μg/mL phosphoglycerate kinase, and 130 μg/mL glyceraldehyde-3-phosphate dehydrogenase. The concentrations of bisphosphoglycerate and phosphate used were not inhibitory, as shown by their inclusion in [γ-^{32}P]ATP assays. The [γ-^{32}P]ATP assays (Avron, 1960) and the pH-stat assays contained 50 mM NaCl, 10 mM Tris-HCl (pH 8.0), 6 mM $CaCl_2$, and 1 mM EDTA. The Tris-HCl was absent in pH-stat assays. In the [γ-^{32}P]-ATP assays, the amount of [^{32}P]P_i formed was determined at 15-s intervals for 1 min.

Measurement of Exchange at Site 1. Nitrocellulose filters (0.2 μm, BA83, Schleicher & Schuell) bind CF_1 but not free nucleotides. When 100 μL of 0.25 μM CF_1 containing [^3H]ADP at site 1 was passed through a nitrocellulose filter by using an aspirator, 60% of the radioactivity was reproducibly retained by the filter. The radioactivity that was not retained was [^3H]ADP·CF_1 with the same specific radioactivity as that of the original sample. When CF_1 that washed through a filter was refiltered, it behaved identically with the original sample. In the experiments measuring the rate of exchange, site 1 was first labeled with [^3H]ADP (120 000 cpm/nmol) (Bruist & Hammes, 1981). Exchange of nonradioactive ATP for enzyme-bound [^3H]ADP was measured by incubating 200 μL of 0.26 μM labeled heat-activated CF_1 (freed of dissociable nucleotides) with ATP in the NaCl–Tris–EDTA buffer containing 6 mM $CaCl_2$ for 10 s, filtering 100 μL of the solution through a nitrocellulose filter, and immediately washing with 200 μL of 200 mM EDTA–20 mM Tris-HCl (pH 8.0). The filters were dried for 30 min at 110 °C, immersed in 10 mL of ACS scintillation fluid overnight, and counted for radioactivity.

The effect of TNP-ADP occupying site 1 on the enzymatic activity was determined as follows. Heat-activated CF_1 was incubated with a 10-fold or greater excess of TNP-ADP in the NaCl–Tris–EDTA buffer. At given time intervals, 350 μL of the mixture was pipetted onto a 3-mL centrifuge column equilibrated with the same buffer and centrifuged. The sample was passed through two more centrifuge columns to remove all dissociable TNP-ADP and then assayed by the pH-stat or [γ-^{32}P]ATP method. The amount of bound TNP-ADP was determined spectrophotometrically by using an extinction coefficient of 25.4 × 10^3 M^{-1} cm^{-1} at 418 nm (Cerione & Hammes, 1982). In order to show that TNP-ADP is displaced from site 1 during catalytic turnover, TNP-ADP-labeled heat-activated CF_1 was incubated with 200 μM ATP and 6 mM $CaCl_2$ in the NaCl–Tris–EDTA buffer for 1 min and then passed through two centrifuge columns.

Stopped-Flow Experiments. The rapid quenching of fluorescence that occurs when ϵ-ATP binds to CF_1 was mea-

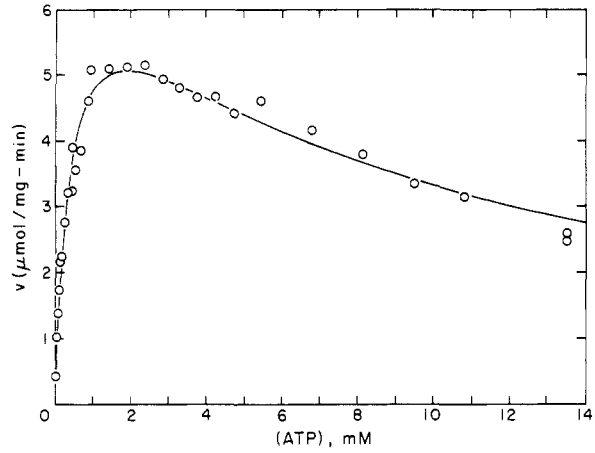

FIGURE 1: Plot of the initial steady-state velocity of ATP hydrolysis by heat-activated CF_1, v, vs. ATP concentration. The initial velocities were measured by using the enzyme-coupled assay at 20 °C. The assays were carried out in 50 mM NaCl, 6 mM DL-glyceraldehyde 3-phosphate, 5 mM Tris-HCl (pH 8.0), 2.5 mM $CaCl_2$, 1.5 mM NAD, 1 mM EDTA, 1 mM P_i, 24 μg/mL phosphoglycerate kinase, 130 μg/mL glyceraldehyde-3-phosphate dehydrogenase, and 7.1–21 μg/mL CF_1. The line was calculated with eq 1 and the parameters k_{cat} = 7.6 μmol/(mg·min), K_m = 430 μM, and K'_I = 8.3 mM.

sured on a Durrum-Gibson stopped-flow spectrophotometer (Dionex Corp.) with a 200-W Hanovia Xe–Hg arc lamp. Site 2 of latent CF_1 was blocked with ATP, and the complex was kept in 40 mM Tris-HCl (pH 8.0), 2.5 mM $MgCl_2$, and 2 mM EDTA to ensure that no ATP dissociated. Just prior to a stopped-flow experiment, the enzyme was passed through a centrifuge column equilibrated with the NaCl–Tris–EDTA buffer. For experiments with heat-activated enzyme, the CF_1 was activated prior to blocking site 2. In the stopped-flow experiments, 0.15 mL of enzyme in the NaCl–Tris–EDTA buffer was mixed with an equal volume of a 10-fold molar excess of ε-ATP in the same buffer containing 12 mM $CaCl_2$. The fluorescence of ε-ATP was excited at 300 nm, and a Corning CSO 51 (350-nm) cutoff filter was put in front of the photomultiplier. No enzyme fluorescence was detected under these conditions. The photomultiplier voltage was adjusted to maintain a 2-V signal for varying ε-ATP concentrations. Fluorescence decay traces were collected in a PDP 11 computer (DEC) via a Biomation 802 transient recorder. The data from 2 to 20 experiments were collected and averaged at each ε-ATP concentration.

Data Analysis. The kinetic data were fit to the desired equations by using a nonlinear least-squares analysis.

Results

Steady-State Kinetics of Nucleotide Hydrolysis. The ATP hydrolysis activity of heat-activated CF_1 is inhibited by CaADP. This inhibition was minimized by utilizing an assay in which ADP is rapidly converted to ATP by phosphoglycerate kinase. Figure 1 shows a plot of the initial rate of ATP hydrolysis vs. the concentration of ATP. At high ATP concentrations, the hydrolysis activity is inhibited as previously observed (Cantley & Hammes, 1975). The substrate inhibition can be accounted for by assuming a low affinity site for ATP which inactivates the enzyme when occupied. The initial steady-state velocity, v, for such a model is

$$\frac{v}{(E_0)} = k_{cat}\left[\frac{(ATP)}{K_m + (ATP)}\right]\left[\frac{K'_I}{K'_I + (ATP)}\right] \quad (1)$$

where k_{cat} is the catalytic rate constant, (E_0) is the total enzyme concentration, K_m is the Michaelis constant, and K'_I is the dissociation constant for ATP binding at the inhibitory site.

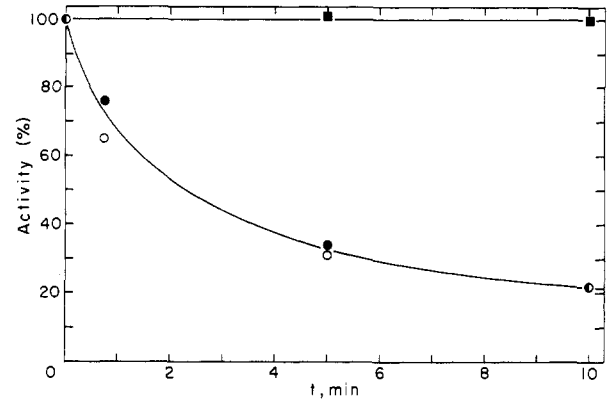

FIGURE 2: Plot of the activity of heat-activated CF_1 vs. the time of incubation of CF_1 with 85 μM ADP and 6 mM $CaCl_2$ in NaCl–Tris–EDTA buffer, pH 8.0, at 20 °C. Aliquots were assayed at the times indicated by the pH-stat technique with 200 μM ATP at pH 8.0. The time course for 3.4 μM CF_1 without site 2 blocked (●) and for 3.8 μM CF_1 with site 2 blocked by MgATP (○) is shown. The initial activity of unblocked CF_1 was 10.8 μmol/(mg·min) and of blocked CF_1 was 8.9 μmol/(mg·min). Unblocked CF_1 was not inhibited by 40 μM ADP with no Ca^{2+} present (■).

The data in Figure 1 were best fit with the parameters k_{cat} = 7.6 μmol/(mg·min), K_m = 430 μM, and K'_I = 8.3 mM. At ATP concentrations below about 40 μM, the initial velocities fall slightly below those predicted by simple Michaelis–Menten kinetics. This observation is discussed later.

For determination of K_m and k_{cat} for various nucleotides and for CF_1 under different conditions, data were obtained only at low nucleotide concentrations where substrate inhibition is not significant. When only ATP concentrations less than 500 μM are considered, the data of Figure 1 fit simple Michaelis–Menten kinetics and give k_{cat} = 5.1 μmol/(mg·min) and K_m = 200 μM. Thus, the quantitative values obtained for K_m and k_{cat} depend slightly on the model assumed and on the range of ATP concentrations considered. At ATP concentrations below 1 mM, the pH-stat and [γ-^{32}P]ATP assay methods give the same results as the enzyme-coupled assay if the ATP is purified to remove contaminating ADP and the assay is carried out for only 1 min. In the enzyme-coupled assays, a free Ca^{2+} concentration of 1.5 mM was used. Higher Ca^{2+} concentrations resulted in precipitation of $Ca_3(PO_4)_2$ at pH 8. Previous binding studies (Bruist & Hammes, 1981) and all other experiments discussed in this work were done with 5 mM free Ca^{2+} present. At this higher free Ca^{2+} concentration, the Michaelis constant for ATP is approximately the same, and k_{cat} increases slightly. The values of both k_{cat} and K_m vary significantly for different enzyme preparations: the range in k_{cat} is 10–20 μmol/(mg·min), and the range in K_m is 70–200 μM at 5 mM free Ca^{2+}.

When heat-activated CF_1 is incubated with ADP in the presence of Ca^{2+}, a slow inactivation of ATP hydrolysis takes place. Neither Ca^{2+} nor ADP alone causes a similar inhibition. The time course of this inactivation is shown in Figure 2. The half-time for the inactivation is about 2.5 min at 85 μM ADP and 5 mM free Ca^{2+}. The rate of inactivation is half-maximal at approximately 10 μM ADP–5 mM Ca^{2+} (data not shown). This inhibition is distinct from the inhibition of the initial velocity by ADP (Cantley & Hammes, 1975).

The steady-state kinetics of hydrolysis were examined for a variety of nucleotides with the pH-stat assay. The fluorescent nucleotide ε-ATP has a Michaelis constant of 119 μM and a catalytic rate constant of 0.153 μmol/(mg·min), while formycin triphosphate has a Michaelis constant of 850 μM and a catalytic rate constant of 0.44 μmol/(mg·min). The chro-

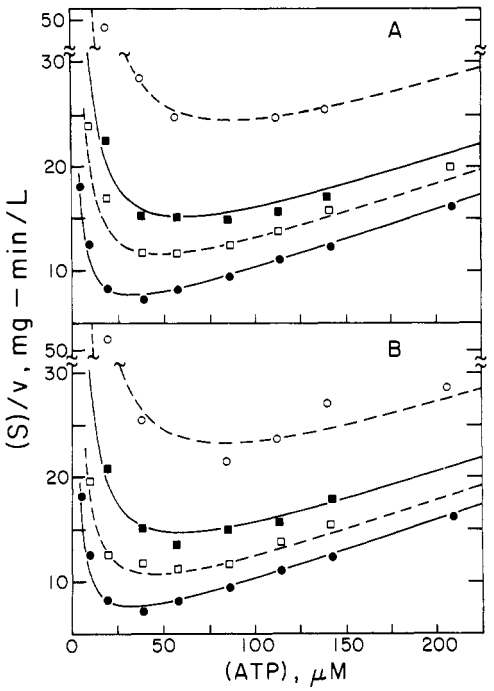

FIGURE 3: Plots of the ATP concentration divided by the initial steady-state velocity of ATP hydrolysis, $(S)/v$, vs. the ATP concentration at various concentrations of the inhibitors TNP-ADP and TNP-ATP. Initial velocities were measured by using the pH-stat technique at pH 8.0. The inhibitor concentrations were corrected for the amount bound to CF_1, and the average concentrations are given. The filled circles (●) show the data in the absence of inhibitors. (A) The concentrations of TNP-ADP were 19 (□), 40 (■), and 99 nM (○). (B) The concentrations of TNP-ATP were 2.1 (□), 5.3 (■), and 13 nM (○). Assays were carried out in 10 mL of 50 mM NaCl, 6 mM $CaCl_2$, and 1 mM EDTA, pH 8.0 at 20 °C, and the CF_1 concentration ranged from 0.6 to 5.1 nM. The lines were calculated with eq 9 and the parameters k_3 = 17 μmol/(mg·min), K_1 = 36 μM, K_4 = 29 μM, $K_{I,TNP\text{-}ADP}$ = 16 nM, and $K_{I,TNP\text{-}ATP}$ = 2.3 nM.

mophoric nucleotides TNP-ATP and 6-mercaptopurine riboside triphosphate are not substrates for CF_1 as measured by the pH-stat assay. However, TNP-ATP and TNP-ADP are both potent inhibitors of the enzyme. Figure 3A,B shows plots of $(ATP)/v$ vs. (ATP) for varying concentrations of TNP-ADP (Figure 3A) and TNP-ATP (Figure 3B). (For clarity, not all of the data are presented.) The curvature of the lines at fixed concentrations of the inhibitor indicates that the inhibition is not simple. However, at high ATP concentrations, the data approach the pattern expected for competitive inhibition. Despite this strong inhibition at nanomolar concentrations of TNP nucleotides, equilibrium dissociation constants for TNP-ADP determined by fluorescence quenching (Cerione & Hammes, 1982) and by forced dialysis (R. Cerione, unpublished results) are in the micromolar range. A model which can explain both the kinetic and binding data is presented later.

The steady-state kinetics of heat-activated CF_1 are not altered when ATP is present at site 2. The inhibition of CF_1 by prior incubation with CaADP also was not altered when this site was occupied (Figure 2). No [^{3}H,γ-^{32}P]ATP was lost from the MgATP site when 1.3 μM heat-activated CF_1 was incubated for 1 h with 5 mM free Ca^{2+} and 40 μM ADP. These experiments demonstrate that the MgATP site is not the site of action for CaADP inhibition and does not play an obvious role in the regulation of ATP hydrolysis.

Kinetic Properties of Site 1. Previous experiments have shown that the rate of exchange of ATP or ADP into site 1 is dependent on the nucleotide concentration (Carlier & Hammes, 1979) and that the rate of exchange is much slower

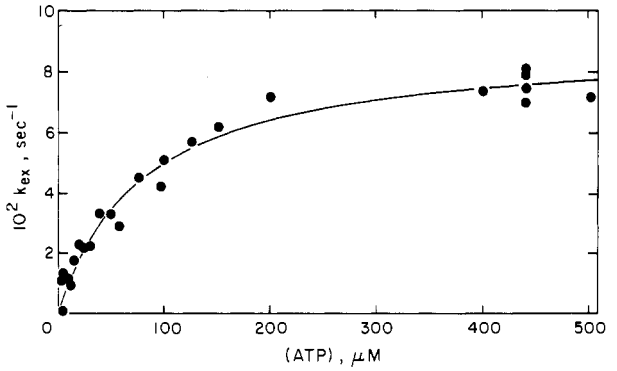

FIGURE 4: Plot of the initial rate of exchange of [^{3}H]ADP from site 1 of heat-activated CF_1, k_{ex}, vs. the ATP concentration. The experiments were carried out in NaCl–Tris–EDTA buffer, pH 8.0, containing 6 mM $CaCl_2$ and 83–93 μg/mL CF_1 at 20 °C. Rates were measured with the nitrocellulose filter assay and calculated by use of eq 2. The line was calculated with the Michaelis–Menten equation and the parameters K_m = 80 μM and k_{cat} = 0.090 s^{-1}.

Table I: Incorporation of TNP-ADP into Heat-Activated CF_1[a]

time (min)	0[b]	0.5	6.5	13	40	270
TNP-ADP/CF_1		0.19	0.33	0.45	0.62	0.90
activity (%)[c]	100	96	68	57	45	40

[a] Heat-activated CF_1 (10 μM) was incubated with 157 μM TNP-ADP in the NaCl–Tris–EDTA buffer for the time indicated and then passed through three centrifuge columns equilibrated with the same buffer. [b] Before the addition of TNP-ADP. [c] Assayed at pH 8.0 by the pH-stat method in 200 μM ATP, 50 mM NaCl, 6.2 mM $CaCl_2$, and 1 mM EDTA. 100% activity corresponds to 7.0 μmol/(mg·min).

than catalysis (Bruist & Hammes, 1981). Here we present a more careful study of the rate of nucleotide exchange as a function of ATP concentration. The nitrocellulose filter assay allows much lower concentrations of CF_1 to be used, thus reducing problems caused by rapid ATP depletion and ADP production. Initial rates of exchange were obtained by measuring the amount of [^{3}H]ADP retained in site 1 of labeled heat-activated CF_1 10 s after mixing with nonradioactive ATP. The loss of [^{3}H]ADP was assumed to follow an exponential decay, and the initial rates of loss, k_{ex}, were calculated by using

$$k_{ex} = (\ln A_0 - \ln A_{10})/10 \quad (2)$$

where A_0 is the initial specific radioactivity of the CF_1 and A_{10} is the specific radioactivity after the 10-s incubation with ATP. At the highest ATP concentration, the specific radioactivity decreased 53% in 10 s. The rate constant, k_{ex}, is plotted vs. the concentration of ATP in Figure 4. These data were fit to the Michaelis–Menten equation (eq 1 with K'_I = ∞). The best fit parameters are K_m = 80 μM and k_{cat} = 0.090 s^{-1}. Although the maximum exchange rate is much lower than the hydrolysis rate at the catalytic site, the Michaelis constant is similar for both activities, suggesting that exchange may be coupled to ATP hydrolysis.

Further evidence for communication between site 1 and the active site is that the presence of TNP-ADP in site 1 inhibits ATP hydrolysis. The exchange of TNP-ADP for [^{3}H]ADP in site 1 has been previously demonstrated (Cerione & Hammes, 1982). Table I shows the results of an experiment in which 10 μM heat-activated CF_1 was incubated with 157 μM TNP-ADP, and samples were analyzed for TNP-ADP incorporation and specific activity (by the pH-stat assay) at various times. The TNP-ADP exchanges into site 1 with a half-time of about 8 min, and the specific activity of the enzyme decreases with increasing TNP-ADP incorporation. Approximately 40% of the activity remains when 1 TNP-

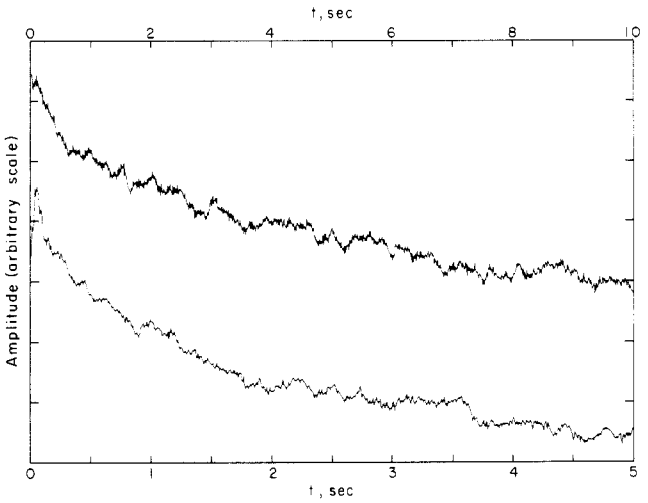

FIGURE 5: Typical plots of the fluorescence vs. time obtained in the stopped-flow studies for the binding of ϵ-ATP to CF_1. The upper trace shows the initial 10 s of 5.2 μM heat-activated CF_1 reacting with 50 μM ϵ-ATP. The lower trace shows the initial 5 s of 4.9 μM latent CF_1 reacting with 50 μM ϵ-ATP. The experiments were carried out in 6 mM $CaCl_2$ and NaCl–Tris–EDTA buffer, pH 8.0, at 20 °C.

ADP/CF_1 is incorporated. A separate experiment showed that incubation of heat-activated CF_1 containing 0.8 TNP-ADP/CF_1 with 200 μM ATP and 5 mM free Ca^{2+} for 1 min (assay conditions) resulted in the release of 0.5 TNP-ADP/CF_1. Thus, the activities in Table I do not approach zero as the TNP-ADP:CF_1 ratio goes to 1 because TNP-ADP is released from the enzyme during the assay. If the loss of TNP-ADP from CF_1 is approximated to be linear with time, enzyme starting with 0.8 and finishing with 0.3 TNP-ADP/CF_1 after 1 min would be 45% active if the enzyme containing bound TNP-ADP is assumed to be completely inactive. Similar behavior was observed with TNP-ATP; however, the TNP-ATP may be hydrolyzed to TNP-ADP in site 1. In the assay of CF_1 with the greatest amount of TNP-ADP bound in Table I, the total concentration of TNP-ADP was 10 nM. The steady-state kinetic studies reported above indicate this concentration of free TNP-ADP would cause about 10% inhibition. To be absolutely certain that the observed inhibition was not due to the released TNP-ADP acting at another site, the more sensitive [γ-^{32}P]ATP assay also was used. When the total TNP-ADP concentration was 1.0 nM, enzyme initially containing 0.93 TNP-ADP/CF_1 had 54% of the control activity in a 1-min assay. Thus, the simplest interpretation of these results is that the binding of TNP-ADP at site 1 inactivates the enzyme.

Kinetics of Nucleotide Binding at Site 3. The stopped-flow technique was used to study the binding of ϵ-ATP to site 3. The fluorescence of ϵ-ATP or ϵ-ADP is partially quenched upon binding to the dissociable nucleotide binding site (Cerione & Hammes, 1982), and the time course of this fluorescence quenching was studied. As reported above, ϵ-ATP has approximately the same Michaelis constant as ATP, but its turnover number is only about 1% that of ATP. In the stopped-flow experiments, site 2 was blocked with MgATP so that no fluorescence quenching due to binding at this site would be observed. When ϵ-ATP and 12 mM $CaCl_2$ in the NaCl–Tris–EDTA buffer are mixed with the NaCl–Tris–EDTA buffer containing no enzyme in the stopped-flow spectrophotometer, a small decrease in fluorescence that is complete within 0.15 s is observed. Therefore, the first 0.15 s of the fluorescence decay traces was not included in the data analysis.

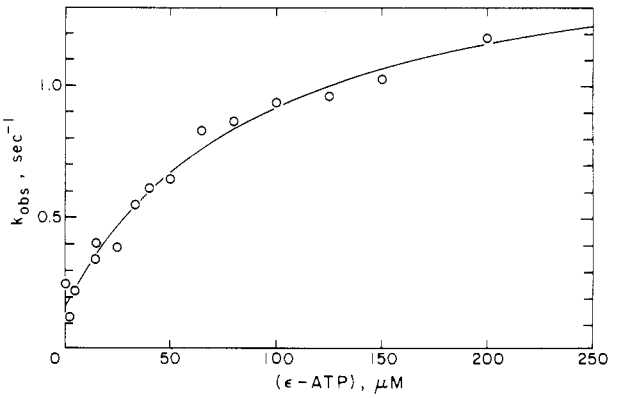

FIGURE 6: Plot of the first-order rate constant associated with the binding of ϵ-ATP to latent CF_1, k_{obsd}, vs. the ϵ-ATP concentration. The CF_1 concentration was one-tenth of the ϵ-ATP concentration, and the experiments were carried out in 6 mM $CaCl_2$ and NaCl–Tris–EDTA buffer, pH 8.0, at 20 °C. The values for k_{obsd} were obtained by using eq 3. The line was calculated with eq 5 and the parameters k_{-2} = 0.15 s^{-1}, k_2 = 1.5 s^{-1}, and K_s = 92 μM.

Figure 5 shows a typical time course of the fluorescence quenching which results when latent CF_1 is mixed with a 10-fold excess of ϵ-ATP in the presence of Ca^{2+}. The initial fluorescence quenching is well described by a single exponential plus a constant:

$$F_t = A_1 e^{-k_{obsd}t} + A_2 \quad (3)$$

where F_t is the fluorescence at time t, A_1 and A_2 are amplitude parameters, and k_{obsd} is the rate constant for the reaction. A further quenching of fluorescence occurs at much longer times ($t_{1/2} \simeq 50$ s). This process is much slower than the rate of ϵ-ATP hydrolysis by the enzyme and was not investigated further. The slow process did not influence the measurement of the fast process at ϵ-ATP concentrations below 200 μM. Figure 6 shows a plot of k_{obsd} vs. the concentration of ϵ-ATP obtained from analysis of the first 5 s of the reaction according to eq 3. The points describe a hyperbola, and a simple mechanism consistent with the data is

$$\epsilon\text{-ATP} + CF_1 \overset{K_s}{\rightleftharpoons} X_1 \underset{k_{-2}}{\overset{k_2}{\rightleftharpoons}} X_2 \xrightarrow{k_3} CF_1 + \epsilon\text{-ADP} + P_i \quad (4)$$

In eq 4, K_s is an equilibrium dissociation constant, the k_i's are rate constants, and X_1 and X_2 are different conformations of the enzyme–substrate complex; the fluorescence of X_2 is less than that of X_1. The step characterized by k_3 represents catalysis and occurs slowly with latent CF_1. If the formation of X_1 occurs very rapidly relative to the rate of formation of X_2, and the concentration of ϵ-ATP is much greater than the enzyme concentration

$$k_{obsd} = k_{-2} + k_2/[1 + K_s/(\epsilon\text{-ATP})] \quad (5)$$

The best fit to this equation of the data in Figure 6 gives k_{-2} = 0.15 s^{-1}, k_2 = 1.5 s^{-1}, and K_s = 92 μM. The line in Figure 6 has been calculated with these parameters and eq 5. The value of k_2 is greater than the turnover number for ϵ-ATP hydrolysis, 0.8 s^{-1}; therefore, the formation of X_2 could be part of the catalytic process. The overall dissociation constant, K_{obsd}, for ϵ-ATP binding to the enzyme in terms of the mechanism of eq 5 is

$$K_{obsd} = K_1/(1 + k_2/k_{-2}) \simeq 8\ \mu M \quad (6)$$

This value is comparable to that obtained by fluorescence titration for ϵ-ADP binding to the enzyme (2 μM; Cerione & Hammes, 1982). The time course for fluorescence quenching becomes more complex when heat-activated enzyme is used (see Figure 5). A single-exponential decay (eq 3) does not

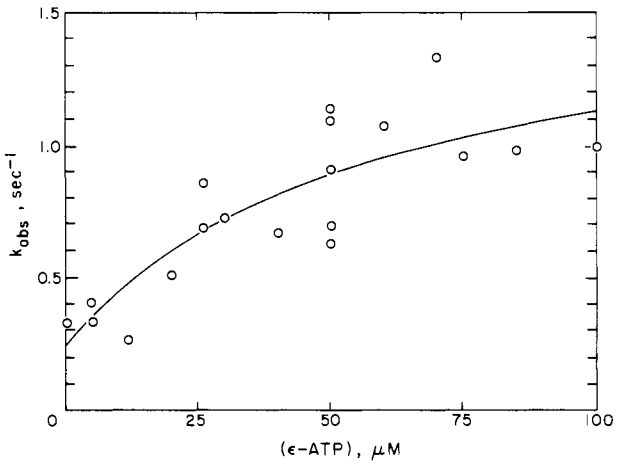

FIGURE 7: Plot of the first-order rate constant associated with the binding of ϵ-ATP to heat-activated CF_1, k_{obsd}, vs. the ϵ-ATP concentration. The CF_1 concentration was one-tenth of the ϵ-ATP concentration, and the experiments were carried out in 6 mM $CaCl_2$ and NaCl–Tris–EDTA buffer, pH 8.0, at 20 °C. The values for k_{obsd} were obtained by using eq 7. The line was calculated with eq 5 and the parameters $k_{-2} = 0.24$ s^{-1}, $k_2 = 1.4$ s^{-1}, and $K_s = 57$ μM.

describe the data. At least one additional exponential is required to fit the data. Unfortunately, the magnitudes of the two time constants were not sufficiently different to allow the fluorescence decay traces to be resolved unambiguously into two exponential components. Since the rate constant characteristic of the slow process is clearly less than the turnover number, no attempt was made to measure it quantitatively. The slow process can be approximated as a negatively sloping line at early times in the quenching process. (A linear time dependence is the first term in the Taylor expansion of an exponential.) There, the first 10 s of the time course of fluorescence quenching accompanying ϵ-ATP binding to heat-activated CF_1 was fit to

$$F_t = A_1 e^{-k_{obsd}t} + A_2 t + A_3 \quad (7)$$

At ϵ-ATP concentrations above 100 μM, k_{obsd} could not be reliably obtained from the data. Figure 7 shows a plot of k_{obsd} as a function of the ϵ-ATP concentration. The data are rather scattered because of the approximate data analysis, but the concentration dependence of k_{obsd} is similar to that obtained with the latent enzyme. When the data are fit to eq 5, the following parameters are obtained: $k_{-2} = 0.24$ s^{-1}, $k_2 = 1.4$ s^{-1}, and $K_s = 57$ μM. The line in Figure 7 has been calculated with eq 5 by assuming these parameters. If K_s was fixed at 92 μM (the value obtained with latent CF_1), the sum of squared errors for the fit increased only 2% and gave $k_{-2} = 0.28$ s^{-1} and $k_2 = 1.7$ s^{-1}. Thus, essentially the same results are obtained for latent and heat-activated enzymes. When heat-activated CF_1 reacts with ϵ-ATP, the hydrolysis step characterized by k_3 in eq 4 also occurs.

Although the nature of the slower fluorescence quenching has not been characterized, it very likely is due to the slow exchange of ϵ-ADP into site 1. This is characterized by a large fluorescence quenching (Cerione & Hammes, 1982) and occurs much more rapidly with heat-activated enzyme than with latent enzyme.

Model for ATP Hydrolysis

The Model. A mechanism now is presented which can quantitatively account for the results reported here, as well as other observations in the literature. In this mechanism, site 1 is postulated to be a regulatory site: the enzyme is inactive when this site is occupied by ADP, TNP-ADP, or TNP-ATP. The catalytic site is postulated to be site 3: occupation of this site by a substrate permits rapid nucleotide dissociation from site 1.

Steady-State Kinetics. The dependence of the initial steady-state velocity on substrate, TNP-ATP, and TNP-ADP concentrations (cf. Figure 3) can be explained in terms of the following mechanism:

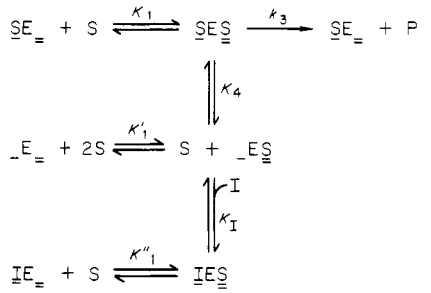

(8)

In this mechanism, the K_i values are equilibrium dissociation constants, the k_i values are rate constants, S is the substrate, P represents the products, and I is an inhibitor. The enzyme is represented as $-E_=$ where $-$ is the regulatory site (site 1) and $=$ is the catalytic site (site 3). Dissociation and association at site 1 can only occur if the catalytic site is occupied, and only the species SES can break down to give products. In analyzing the steady-state kinetic data, we made the assumption that $K_1 = K'_1 = K''_1$ and that all reactions are in rapid equilibrium prior to the step characterized by k_3. For this case, the initial steady-state velocity is

$$\frac{v}{(E_0)} = \frac{k_3(S)}{K_1 + [K_4 + K_1K_4/(S)][1 + (I)/K_I] + (S)} \quad (9)$$

(The form of the rate equation is identical if the steady-state approximation is assumed rather than rapid equilibrium.) This equation predicts that a plot of v vs. (S) should be sigmoidal at low concentrations, or alternatively a plot of (S)/v vs. (S) should be nonlinear, as is observed (Figure 3). The cooperative behavior becomes apparent at very low substrate concentrations and is enhanced in the presence of an inhibitor. For most kinetic studies, the range of substrate concentrations is such that deviations from Michaelis–Menten kinetics are minor. If the apparent Michaelis constant is defined as the substrate concentration at which the initial velocity is one-half the maximum velocity, the apparent Michaelis constant is equal to $^1/_2[K_1 + K_4 + (K_1^2 + 6K_1K_4 + K_4^2)^{1/2}]$. The data in Figure 3 (and other data not shown) were fit simultaneously to eq 9; the unbound inhibitor concentrations were used for this analysis. The best fit parameters are $k_3 = 17$ μmol/(mg·min) (108 s^{-1}), $K_1 = 36$ μM, $K_4 = 29$ μM, $K_{I,TNP\text{-}ADP} = 16$ nM, and $K_{I,TNP\text{-}ATP} = 2.3$ nM. The lines in Figure 3 have been calculated with these parameters and eq 9. Nanomolar inhibition constants for TNP-ATP and TNP-ADP have also been reported for the mitochondrial coupling factor (Grubmeyer & Penefsky, 1981). The possibilities that $K_1 \neq K'_1 \neq K''_1$ or that -ES and IES also break down to give products cannot be excluded; however, the data are well fit without the additional parameters which would be required. The mechanism predicts that very tight binding of TNP-ADP and TNP-ATP to site 1 would not be observed in the absence of substrate. This is a kinetic rather than a thermodynamic restriction. In fact, the smallest dissociation constant observed for TNP-ADP in the absence of substrate is in the micromolar range when only short time incubations are used (Cerione & Hammes, 1982).

ADP Inhibition. The inhibition of the initial steady-state velocity by ADP has been previously studied (Cantley & Hammes, 1975). The earlier data are well fit by eq 9 with

K_1 = 990 μM, K_4 = 69 μM, $K_{I,ADP}$ = 6.2 μM, and k_3 = 4.2 μmol/(mg·min). The difference between these values of k_3, K_1, and K_4 and those obtained in this work reflects different assay conditions and the slow inactivation of the enzyme caused by CaADP in the earlier work.

Substrate Inhibition. Substrate inhibition can occur with the mechanism in eq 8 if $\underline{E}\underline{S}$ breaks down to give products much more rapidly than $\underline{S}\underline{E}\underline{S}$. However, with this assumption, the positive cooperativity observed for the substrate in the presence of inhibitors cannot be obtained while simultaneously fitting the observed substrate inhibition. The best way to fit the substrate inhibition data is to assume a separate binding site for substrate which produces inhibition as in eq 1. This site has a dissociation constant of about 8 mM, and the steady-state data analyzed in terms of eq 9 were obtained at substrate concentrations less than 250 μM. Therefore, inclusion of this additional inhibition in the mechanism does not significantly alter the values of the kinetic parameters.

Stopped-Flow Studies of ϵ-ATP Binding. The binding of ϵ-ATP to site 3 of both latent and heat-activated CF_1 is consistent with the mechanism in eq 4. No significant difference in kinetic parameters for the two enzyme forms was observed, but the data for the heat-activated enzyme are only semiquantitative. If site 3 is assumed to be the catalytic site, the stopped-flow data can be incorporated into the mechanism in eq 8 by assuming the two-step binding mechanism in eq 4 represents the initial binding steps in eq 8. Specifically, the two-step binding would represent the step characterized by the equilibrium dissociation constant K''_1, since CF_1 initially is inhibited by ADP bound to site 1. Nucleotide exchange probably occurs after the conformational change since heat-activated CF_1 can exchange nucleotides much faster than latent CF_1. When all of the initial binding steps in eq 8 are replaced by the two-step mechanism of eq 4 and the values of K_s, k_2, and k_{-2} are independent of the species present in site 1, $k_{cat} = k_2k_3/(k_{-2} + k_2 + k_3)$. Since for ϵ-ATP k_{cat} = 0.83 s^{-1}, k_{-2} = 0.15 s^{-1}, and k_2 = 1.5 s^{-1}, the value of k_3 is 2 s^{-1}. The apparent Michaelis constant is a complex function of the rate constants but is approximately equal to $K_sk_3/(k_2 + k_3) + K_4k_2/(k_2 + k_3)$ when k_{-2} is small relative to k_2 and k_3. Since K_m = 120 μM and K_s = 92 μM, the value of K_4 can be estimated to be 150 μM.

Thus, the stopped-flow studies are consistent with the general mechanism in eq 8 if it is extended to include a two-step binding mechanism for the initial interaction of ϵ-ATP with site 3 of the enzyme. The relevance of this extended mechanism for ATP hydrolysis is not known, but a similar mechanism seems very likely. If such is the case, the rate constants corresponding to k_2 and k_3 would be greatly increased for ATP.

Nucleotide Exchange at Site 1. The rate constant for the dissociation of ADP from site 1 during catalysis reaches a limiting value of 0.09 s^{-1}, and the Michaelis constant for ATP associated with this process is 80 μM. In terms of the mechanism in eq 8, this corresponds to ADP being the inhibitor in the species $\underline{I}\underline{E}_=$ and permitting only an intermediate with the composition $\underline{I}\underline{E}\underline{S}$ to dissociate ADP at a significant rate. The actual rate-determining step could be a conformational change such as that characterized by k_2 in the stopped-flow studies, or dissociation directly from an intermediate such as X_1. Regardless of which step is rate determining, the dissociation of ADP occurs much more rapidly during catalysis. This is consistent with the findings that the exchange of nucleotides at site 1 occurs much more slowly with latent CF_1 than with heat-activated CF_1 (Carlier & Hammes, 1979; Bruist & Hammes, 1981) and that TNP-ATP, which does not appear to be a substrate, exchanges into site 1 of heat-activated CF_1 much more slowly than ATP.

Since isolated CF_1 has ADP at site 1, it would be expected to be inactive until the ADP dissociates. This is a possible explanation for the lag in ATP hydrolysis that is observed after rapid mixing of lettuce CF_1 and ATP (Carmeli et al., 1978, 1981). The lag is characterized by a rate constant of 1 s^{-1}, which is 10 times as large as the rate constant for ADP dissociation obtained in this work with spinach CF_1. The correspondence between these rate constants for the same enzyme under identical conditions remains to be determined. Since the enzyme is postulated to be most active with ATP at site 1 and isolated enzyme always has ADP at site 1, site 1 may have a weak ATPase activity. This activity could serve as an important additional regulator of CF_1.

Discussion

The mechanism proposed for ATP hydrolysis and its regulation provides a framework that accounts for the results of many diverse experiments. While it is similar in concept to the mechanism previously proposed to account for the ADP inhibition of ATP hydrolysis (Cantley & Hammes, 1975), it is now more precisely defined, in both kinetic and structural terms. The steady-state kinetic studies have now been done under conditions which eliminate inhibition due to ADP contamination of the ATP and the slow inactivation due to CaADP. Moreover, a variety of substrates and inhibitors has been examined. The apparent Michaelis constant for CaATP reported here is significantly smaller than that previously observed (Vambutas & Racker, 1965; Cantley & Hammes, 1975), but is similar to the value found for MgATP hydrolysis by the membrane-bound enzyme (70 μM; Franek & Strotmann, 1981). Three nucleotide binding sites on CF_1 have been well characterized (Bruist & Hammes, 1981). A fourth site, with a very large dissociation constant for MgATP (8 mM), is proposed to account for the inhibition observed at high substrate concentrations. The evidence for site 1 being a regulatory site is quite compelling. The function of site 2 is not known since occupation of this site by MgATP has no observable effect on the kinetic properties of the enzyme. Since this site is very likely occupied by CaATP under normal assay conditions, its occupation could be essential for catalytic activity. (The equilibrium dissociation constant for CaADP binding to this site is about 4 μM; Bruist & Hammes, 1981). All of the available data are consistent with site 3 being the catalytic site; however, direct proof is still lacking. The binding site for CaADP associated with the slow inhibition of ATP hydrolysis has not yet been identified.

The proposed mechanism also is consistent with studies of ATP hydrolysis in chloroplasts. The transient light-induced ATPase activity of membrane-bound CF_1 in chloroplasts has been shown to be inhibited when ADP binds to a tight binding site on CF_1 (Dunham & Selman, 1981; Strotmann et al., 1981). Furthermore, the lifetime of the transient ATPase activity is lengthened by the addition of ATP and shortened by the addition of ADP. This ADP- and ATP-binding regulatory site would correspond to site 1 of isolated CF_1. Some modifications of the model are necessary when ATP synthesis is considered. Since the enzyme is postulated to be active only when ATP is bound at site 1 and isolated CF_1 appears to have a higher affinity for ADP than ATP at site 1, the enzyme would be expected to be inactive under conditions necessary for ATP synthesis. When a proton gradient is introduced across the chloroplast membrane, ADP tightly bound to the coupling factor is released into the medium (Bickel-Sandkötter

& Strotmann, 1976; Magnusson & McCarty, 1976). Therefore, conformational changes induced in the enzyme by energization of the membrane may change the relative affinity of site 1 for ATP and ADP. This possibility is supported by the observation that 3′-(1-naphthoyl)-ATP appears to be a much better inhibitor of ATP hydrolysis than of ATP synthesis by the membrane-bound enzyme (Franek & Strotmann, 1981). The phosphate ion also may play a regulatory role. The light-induced transient ATPase activity of membrane-bound CF_1 is stabilized by phosphate (Carmeli & Lifshitz, 1972); perhaps phosphate alleviates the ADP inhibition. Finally, the species of enzyme with site 1 unoccupied (_ES) might have significant activity; this could be especially important in the initial stages of synthesis when the concentration of ATP may be too low for site 1 to be occupied.

The model proposed is the simplest that accounts for all of the results discussed. Another possible model is that sites 1 and 3 alternate as the catalytic sites (Hackney et al., 1979). In this model, site 1 becomes a catalytic site after inhibitory ADP is released. The evidence against this mechanism is that the measured rate of dissociation of ADP from site 1 is slow ($k_{cat} \simeq 0.1\ s^{-1}$) relative to turnover ($k_{cat} \simeq 100\ s^{-1}$). If site 1 is a catalytic site, the rate constant for nucleotide dissociation must be at least as large as the turnover number during catalysis. However, the possibility exists that only a small fraction of the enzyme is active while ADP dissociation is being measured and that the dissociation rate accelerates after the initial dissociation of ADP. A finding frequently cited in support of the alternating site mechanism is the dependence on substrate concentration of the number of water oxygens which exchange into product phosphate during a single turnover (Hackney et al., 1979). The model proposed here predicts a dependence similar to that of the alternating site mechanism if both SES and _ES lead to species in which the oxygens of the terminal phosphate of bound ATP can exchange with water. Obviously, more experiments are required to distinguish these and other models. However, the concepts of the proposed mechanism appear to be consistent with currently available information. The conformational changes observed in isolated CF_1 may be eventually related to the proton translocation steps proposed for the membrane-bound coupling factor (Dewey & Hammes, 1981).

References

Avron, M. (1960) *Biochim. Biophys. Acta 40*, 257.

Baird, B. A., & Hammes, G. G. (1979) *Biochim. Biophys. Acta 549*, 31.

Bickel-Sandkötter, S., & Strotmann, H. (1976) *FEBS Lett. 65*, 102.

Binder, A., Jagendorf, A., & Ngo, E. (1978) *J. Biol. Chem. 253*, 3094.

Boyer, P. D., Chance, B., Ernster, L., Mitchell, P., Racker, E., & Slater, E. C. (1977) *Annu. Rev. Biochem. 46*, 955.

Bruist, M. F., & Hammes, G. G. (1981) *Biochemistry 20*, 6298.

Bücher, T. (1947) *Biochim. Biophys. Acta 1*, 292.

Cantley, L. C., Jr., & Hammes, G. G. (1975) *Biochemistry 14*, 2968.

Carlier, M.-F., & Hammes, G. G. (1979) *Biochemistry 18*, 3446.

Carmeli, C., & Lifshitz, Y. (1972) *Biochim. Biophys. Acta 267*, 86.

Carmeli, C., Lifshitz, Y., & Gutman, M. (1978) *FEBS Lett. 89*, 211.

Carmeli, C., Lifshitz, Y., & Gutman, M. (1981) *Biochemistry 20*, 3940.

Cerione, R. A., & Hammes, G. G. (1982) *Biochemistry 21*, 745.

Cross, R. L. (1981) *Annu. Rev. Biochem. 50*, 681.

Dewey, T. G., & Hammes, G. G. (1981) *J. Biol. Chem. 256*, 8941.

Dunham, K. R., & Selman, B. R. (1981) *J. Biol. Chem. 256*, 212.

Farron, F. (1970) *Biochemistry 9*, 3823.

Farron, F., & Racker, E. (1970) *Biochemistry 9*, 3829.

Franek, U., & Strotmann, H. (1981) *FEBS Lett. 126*, 5.

Grubmeyer, C., & Penefsky, H. S. (1981) *J. Biol. Chem. 256*, 3718.

Hackney, D. D., Rosen, G., & Boyer, P. D. (1979) *Proc. Natl. Acad. Sci. U.S.A. 76*, 3646.

Lien, S., & Racker, E. (1971) *Methods Enzymol. 28*, 547.

Magnusson, R. P., & McCarty, R. E. (1976) *J. Biol. Chem. 251*, 7417.

Penefsky, H. S. (1977) *J. Biol. Chem. 252*, 2891.

Strotmann, H., Bickel-Sandkötter, S., Franek, U., & Gerke, V. (1981) *Energy Coupling in Photosynthesis* (Selman, B. R., & Selman-Reimer, S., Eds.) p 187, Elsevier/North-Holland.

Vambutas, V. K., & Racker, E. (1965) *J. Biol. Chem. 240*, 2660.